

See discussions, stats, and author profiles for this publication at: <https://www.researchgate.net/publication/221902129>

Halogenated xenon cyanides ClXeCN, ClXeNC, and BrXeCN

ARTICLE in INORGANIC CHEMISTRY · MARCH 2012

Impact Factor: 4.76 · DOI: 10.1021/ic3002543 · Source: PubMed

CITATIONS

28

READS

49

5 AUTHORS, INCLUDING:



Antti Lignell

California Institute of Technology

44 PUBLICATIONS 848 CITATIONS

SEE PROFILE



Alexandra V. Domanskaya

41 PUBLICATIONS 466 CITATIONS

SEE PROFILE



Markku Rasanen

University of Helsinki

268 PUBLICATIONS 7,129 CITATIONS

SEE PROFILE

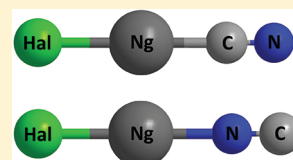
Halogenated Xenon Cyanides ClXeCN, ClXeNC, and BrXeCN

Teemu Arppe, Leonid Khriachtchev,* Antti Lignell,[†] Alexandra V. Domanskaya,[‡] and Markku Räsänen

Department of Chemistry, P.O. Box 55, FIN-00014 University of Helsinki, Finland

S Supporting Information

ABSTRACT: We report on the preparation and characterization of three new noble-gas molecules ClXeCN, ClXeNC, and BrXeCN. These molecules are synthesized by 193 nm photolysis and thermal annealing of ClCN and BrCN in a xenon matrix. The absorption spectra are measured in the mid- and far-infrared regions, and the assignment is supported by isotope substitution and quantum chemical calculations at the B3LYP and MP2 levels of theory. The present results demonstrate a way to prepare other noble-gas molecules of this type.



■ INTRODUCTION

The noble-gas (Ng) chemistry started with the synthesis of xenon hexafluoroplatinate by Neil Bartlett in 1962.¹ A large number of compounds with Xe and Kr atoms have been reported later, XeF₂ and KrF₂ being important for synthetic work.^{2–4} These achievements have greatly benefited from studies using cryogenic techniques. For example, noble-gas halides KrF₂, XeCl₂, and XeClF were prepared and identified in matrix-isolation experiments.^{5,6}

Chemical synthesis at cryogenic temperatures led to the discovery of noble-gas hydrides with the general formula HNgY, where Y is an electronegative fragment, HXeOBr being the last identified molecule.^{7–10} In this way, the first neutral ground-state molecule with argon (HArF) was prepared.^{11,12} Among these molecules are HXeCN and HXeNC, where xenon is bonded to a cyano or isocyano group, and HKrCN that is the first molecule with the Kr–C chemical bond.¹³ HKrCCH, HXeCCH, HKrC₄H, and HXeC₄H are other examples of experimentally observed noble-gas hydrides with the Ng–C chemical bonds,^{14–17} and HXeNCO possesses the Xe–N bond.¹⁸

The experiments with cyanoacetylene (HCCCN) in noble-gas matrices led to the identification of the HNgCCCN (Ng = Kr and Xe) species.¹⁹ In the same paper, molecules of a different type, HCCNgCN and HCCNgNC (Ng = Ar, Kr, and Xe), were predicted theoretically; however, their experimental observation failed. In this respect, more successful was the work with the HCCF precursor, where, in addition to HKrCCF and HXeCCF hydrides, a molecule of a different type, FKrCCH, was experimentally found.²⁰ As a puzzle of that study, FXeCCH was not observed in the experiments, although it is computationally very stable, similar to HXeF that could not be prepared either despite extensive work in our laboratory. It has been speculated that the strong interaction between Xe and F atoms creates a barrier for the formation of these molecules at low temperatures.²⁰

In the present work, molecules with the formula HalNgY, where Hal is a halogen atom, are studied experimentally and theoretically. We have chosen Hal = Cl and Br, Y = CN, keeping in mind that HXeCN, HXeNC, and HKrCN were previously prepared.¹³ As a result, we report on the

identification of three new noble-gas molecules: ClXeCN, ClXeNC, and BrXeCN.

■ COMPUTATIONAL RESULTS

First, we evaluate the structure and properties of the HalCN and HalNgCN isomers (Hal = Cl and Br, Ng = Kr and Xe) at the MP2 and B3LYP levels of theory using the aug-cc-pVTZ basis set as implemented in Gaussian 09.²¹ A small-core relativistic pseudopotential is used for xenon.²² All optimized structures are linear and correspond to the true minima on the potential energy surface (Figure 1). The bond lengths are given

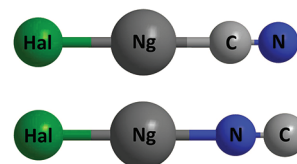


Figure 1. Structure of the HalNgCN isomers (Hal = Cl and Br; Ng = Kr and Xe).

in the Supporting Information (Table S1), the MP2 and B3LYP methods yielding similar results. The partial atomic charges in the HalNgCN isomers were obtained using the natural population analysis (Table 1).²³ The Ng atom carries a positive charge, whereas the halogen atom and the CN group are negatively charged.

The B3LYP energies of the calculated noble-gas molecules with respect to the three-body (3B) asymptote (Hal + Xe + CN) are shown in Table 2. The preferable use of the B3LYP method for the energetic estimates is based on the following. It has been shown that the alternative MP2 method strongly overestimates the stability of noble-gas hydrides HNgY, whereas the B3LYP results are substantially more realistic.²⁴ The accuracy of the calculations can be evaluated by comparing the experimental dissociation energy of HY and the theoretical gap between the (HY + Xe) two-body (2B) and (H + Xe + Y)

Received: February 3, 2012

Published: March 21, 2012

Table 1. Partial Atomic Charges in the HalNgCN Isomers (Hal = Cl and Br; Ng = Kr and Xe) Obtained Using the Natural Population Analysis

	ClXeCN	ClXeNC	BrXeCN	BrXeNC	ClKrCN	ClKrNC	BrKrCN	BrKrNC
Hal	−0.47	−0.37	−0.38	−0.28	−0.37	−0.24	−0.27	−0.14
Ng	+0.86	+0.94	+0.79	+0.85	+0.67	+0.69	+0.59	+0.59
C	−0.06	+0.26	−0.06	+0.24	+0.05	+0.26	+0.05	+0.25
N	−0.34	−0.82	−0.35	−0.81	−0.34	−0.71	−0.36	−0.70

Table 2. B3LYP Energies (in eV) of the HalNgCN and HalCN Isomers (Hal = Cl and Br; Ng = Kr and Xe) with Respect to the 3B Asymptote

	Kr	Xe
Cl + Ng + CN	0	0
ClNgNC	+0.32	−0.90
ClNgCN	−0.35	−1.50
CINC + Ng	−2.60	−2.60
ClCN + Ng	−4.44	−4.44
Br + Ng + CN	0	0
BrNgNC	+0.45	−0.64
BrNgCN	−0.14	−1.20
BrNC + Ng	−2.44	−2.44
BrCN + Ng	−3.99	−3.99

three-body (3B) asymptotes. The error of the calculated dissociation energy of HY is supposed to directly contribute to the overestimation of the stability of the HNgY molecules relative to the 3B asymptote.²⁴ On the other hand, the energy of the molecule with respect to the 3B asymptote is of key importance because the molecule can be formed in a diffusion-controlled reaction at low temperatures only if the 3B asymptote is higher in energy than the resulting molecule. In fact, the B3LYP method gives more accurate values for the dissociation energy of HCN compared to MP2 (error: 0.6 eV versus 1.2 eV), and the coupled cluster CCSD(T) method does not provide much improvement (error: 0.4 eV).²⁴ This difference is connected to the fact that density functional theory (DFT) can better describe open-shell systems (CN radical in the present case) compared to the lower-level perturbation theoretical approaches, such as MP2.²⁴ A similar

situation with theoretical errors presumably occurs for the present case, although we have no experimental data on the dissociation energies of ClCN and BrCN. The B3LYP dissociation energy of ClCN (4.44 eV) is quite close to the CCSD(T) value of 4.27 eV reported by Bhattacharyya et al.²⁵ As expected, the MP2 method with the aug-cc-pVTZ basis set suggests a substantially higher stability (by about 1 eV) of all the studied molecules with respect to the 3B asymptote, which is in agreement with this discussion.

The calculations show that ClXeCN, ClXeNC, and BrXeCN are reliably stable (lower in energy) with respect to the 3B channel; thus, we may expect their formation at low temperatures. On the other hand, the preparation of BrXeNC looks less probable from this point of view because the stabilization energy is comparable with the expected computational error (presumably about 0.6 eV). The calculations indicate that the energies of ClKrNC and BrKrNC are higher than the 3B asymptotes, which makes their preparation improbable. ClKrCN and BrKrCN are also probably too high in energy, taking into account the expected overestimate of their stability at this level of theory. In addition, we calculated a number of other noble-gas cyanides with different halogens and noble-gas atoms. The computationally most stable of the calculated molecules are FXeCN and FXeNC (−2.53 and −1.84 eV relative to the 3B asymptote). Even the krypton molecule FKrCN seems to be stable enough for experimental observation (−1.19 eV), whereas the argon molecule FArCN is unlikely to be prepared (−0.03 eV) as well as the molecules of this type with Hal = I possibly excluding IXeCN (−0.85 eV). All calculated molecules are much higher in energy than the 2B energy [HalCN(NC) + Xe].

Table 3. Calculated and Experimental Vibrational Spectra and ¹³C/¹²C Frequency Shifts^a

	B3LYP		MP2		experiment	
	wavenumber (intensity)	¹³ C/ ¹² C shift	wavenumber (intensity)	wavenumber	¹³ C/ ¹² C shift	
ClCN	2308 (45)	−54	2161 (16)	2211	−52	
	404 (5)	−12	383 (5)	382	−11	
CINC	2153 (90)	−37	2101 (52)	2074	−36	
	242 (0.3)	−3	254 (0.1)			
ClXeCN	2259 (59)	−49	2078 (154)	2145	−47	
	321 (195)	−4	355 (210)	319	−3	
ClXeNC	2112 (458)	−43	2045 (443)	2030	−40	
	339 (201)	−3	384 (258)	343	−3	
BrCN	2289 (27)		2138 (6)	2194		
	366 (4)		355 (4)	347		
BrNC	2142 (126)		2097 (81)	2061		
	216 (0.3)		257 (0.1)			
BrXeCN	2252 (71)		2069 (189)	2139		
	297 (182)		336 (201)	297		
BrXeNC	2110 (458)		2038 (482)			
	313 (152)		369 (233)			

^aWavenumbers and isotopic spectral shifts are in cm^{−1}, and intensities are in km mol^{−1}.

Table 3 presents the harmonic vibrational frequencies of HalXeCN ($\text{Hal} = \text{Cl}$ and Br) isomers and their precursors calculated by the MP2 and B3LYP methods with the aug-cc-pVTZ basis set. Only the most characteristic modes in the range of our measurements are shown (see Table S2 in the Supporting Information for the full spectra and assignment of the modes). The MP2 and B3LYP methods yield consistent vibrational spectra. The $^{13}\text{C}/^{12}\text{C}$ isotope frequency shifts are also evaluated for the Cl-containing species because this isotopic substitution is used in the current work for assignment.

EXPERIMENTAL RESULTS AND ASSIGNMENTS

The ClCN precursor was synthesized from Cl_2 and NaCN using CCl_4 as a solvent, as described in the literature.²⁶ The crude product was pumped at -79°C to remove Cl_2 . Some amount of CCl_4 and HCN remained in the sample. Isotopically substituted Cl^{13}CN was synthesized with the same method from Cl_2 and Na^{13}CN (Icon). BrCN was purchased from Fluka and used without additional purification. The precursor gas was diluted with a noble gas with a ratio of about 1:1000, and the mixture was deposited onto a CsI window (at 30 K for xenon). The infrared spectra were recorded at 9 K with a Bruker Vertex 80 spectrometer using a mercury cadmium telluride (MCT) detector and a KBr beam splitter in the mid-infrared region and a deuterated L-alanine-doped triglycine sulfate (DLATGS) detector and a Mylar beam splitter in the far-infrared region. The matrixes were irradiated with a 193 nm excimer laser (APD, DE202A) at a substrate temperature of 9 K.

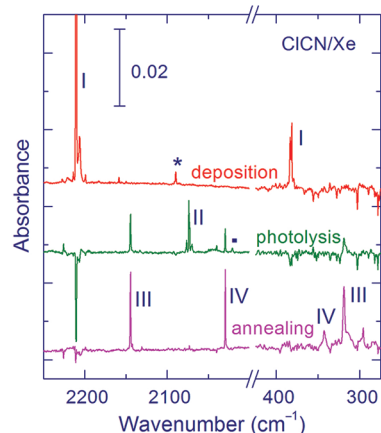


Figure 2. Infrared spectra of ClCN and light-induced and annealing-induced products in a xenon matrix (from top to bottom): after deposition, the result of 193 nm photolysis (difference spectrum with the background after deposition), and the result of annealing at 40 K (difference spectrum with the background after photolysis). The band of HCN is marked with an asterisk, and the band of CN is marked with a dot. The spectra were measured at 9 K. ClCN, ClCN, ClXeCN, and ClXeNC are marked with I, II, III, and IV, respectively.

The absorption bands of ClCN (absorber I) in a xenon matrix are observed at 2211 and 382 cm^{-1} (Figure 2 and Table 3), which is consistent with the literature data on ClCN obtained in argon and krypton matrixes.²⁷ The experimental frequencies reasonably agree with the calculations, including the $^{13}\text{C}/^{12}\text{C}$ frequency shift for the $\text{C}\equiv\text{N}$ stretching mode (experiment: -52 cm^{-1} ; B3LYP: -54 cm^{-1}).

Upon 193 nm photolysis, the intensity of the ClCN bands decreases typically by 20% after 4000 pulses with a pulse energy density of $\sim 15\text{ mJ cm}^{-2}$. The decomposition efficiency is probably limited by self-limitation of photolysis due to rising absorbers.²⁸ As a result of the photolysis, three strong bands appear in the spectral range of the $\text{C}\equiv\text{N}$ stretching mode (Figure 2). One of these bands (2074 cm^{-1} ,

absorber II) is safely assigned to ClNC, the isomer of the precursor ClCN. The splitting of the ClNC band is probably due to different matrix sites. According to our calculations, the $\text{C}\equiv\text{N}$ stretching mode of ClNC is shifted from that of ClCN by -155 cm^{-1} (B3LYP) and -60 cm^{-1} (MP2), whereas the experimental value is -136 cm^{-1} . This assignment agrees with the observations in an argon matrix where the ClNC band at 2074 cm^{-1} is shifted from the ClCN band at 2209 cm^{-1} by -135 cm^{-1} .^{27,29} The ClNC absorption was not found in the far-infrared region, which agrees with the calculations predicting a band at 242 cm^{-1} with a very low intensity of 0.3 km mol^{-1} . The experimental $^{13}\text{C}/^{12}\text{C}$ frequency shift for absorber II (-36 cm^{-1}) is in excellent agreement with the value calculated for ClNC (B3LYP: -37 cm^{-1}). The observed formation of ClNC indicates the Cl + NC in-cage reaction due to a small cage-exit probability of Cl atoms at the available excess energy. After photolysis, HNC (2021 cm^{-1}) formed from the HCN impurity (2089 cm^{-1}) as well as CN radicals (2040 cm^{-1}) are observed. In contrast to the previous reports,¹³ CN radicals show no rotational structure in the spectrum, which is possibly due to the presence of the Cl fragment in the neighborhood.

Two other light-induced bands are observed at 2145 cm^{-1} (absorber III) and 2030 cm^{-1} (absorber IV), and they are assigned to Xe-containing molecules ClXeCN and ClXeNC. It should be noted that some of the noble-gas hydrides, HN_2Y (e.g., HArF , HArCl , HXeNCO , and HXeBr), also appear upon photolysis of HY in noble-gas matrixes, indicating the locality of this process.^{11,18,30,31} The photolysis of ClCN is intuitively an even more local process so that formation of the Xe-containing compounds ClXeCN and ClXeNC upon UV photolysis is an expected observation. The 2145 and 2030 cm^{-1} bands increase in intensity after annealing at 40–50 K (Figure 2), which is accompanied by a decrease of the CN absorption; however, ClCN and ClNC are not recovered upon annealing. The decrease of the CN concentration is consistent with the Cl + Xe + CN (or NC) reaction, which also explains the absence of the recovery of the precursor upon annealing. This model is similar to the formation mechanism of noble-gas hydrides.⁷ Most probably, the formation of the noble-gas compound in annealing is a completely local process without any extensive diffusion of the fragments. Two far-infrared bands at 319 and 343 cm^{-1} are found to correlate with the bands in the mid-infrared region at 2145 and 2030 cm^{-1} , respectively. The ClXeCN and ClXeNC absorptions can be efficiently bleached by UV light, which is characteristic of noble-gas molecules.^{30,32}

We assign the 2145 and 2030 cm^{-1} bands to ClXeCN and ClXeNC, respectively, based on the calculations. In the calculated spectra, the $\text{C}\equiv\text{N}$ stretching mode of ClXeNC is shifted from that of ClXeCN by -147 cm^{-1} (B3LYP) and -33 cm^{-1} (MP2), whereas the experimental value is -115 cm^{-1} . The corresponding bands in the far-infrared region (319 and 343 cm^{-1}) are in agreement with this assignment (B3LYP: 321 and 339 cm^{-1}). The $^{13}\text{C}/^{12}\text{C}$ frequency shift for the $\text{C}\equiv\text{N}$ stretching mode fully supports our assignments; indeed, the experimental isotope shifts for ClXeCN and ClXeNC (-47 and -40 cm^{-1}) are in good agreement with the theory (B3LYP: -49 and -43 cm^{-1}). The $\text{C}\equiv\text{N}$ stretching frequency of ClXeNC (2030 cm^{-1}) is close to the corresponding value of HXeNC (2044 cm^{-1}),¹³ which also supports the assignment. The $\text{C}\equiv\text{N}$ stretching frequency of HXeNC has not been experimentally reported so that we cannot compare it with the value for ClXeNC.

The calculations suggest that the ClXeCN isomer is formed in larger amounts than ClXeNC. Indeed, the absorption intensity of the $\text{C}\equiv\text{N}$ stretching band predicted for ClXeNC is higher by a factor of 7.8 (B3LYP) and 2.9 (MP2), whereas the corresponding experimental bands of ClXeCN and ClXeNC are similar in intensity. In accord, the experimental far-infrared band of ClXeCN is much stronger than that of ClXeNC, whereas the calculated absorption intensities are similar by both B3LYP and MP2. The less efficient formation of the ClXeNC isomer is not directly connected with its lower calculated stability compared to the other isomer (Table 2), but it may originate from different reaction radii and barriers.

Now we describe the results with the other precursor BrCN. The bands of BrCN (absorber V) are observed in a xenon matrix at 2194 and 347 cm^{-1} (Figure 3), in agreement with the literature data on this

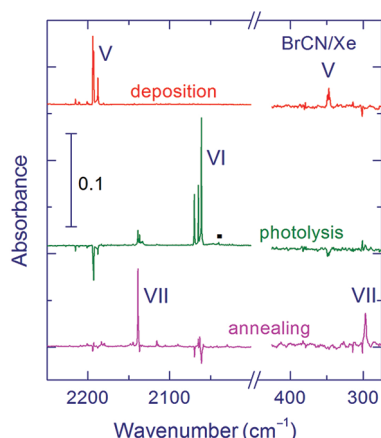


Figure 3. Infrared spectra of BrCN and light-induced and annealing-induced products in a xenon matrix (from top to bottom): after deposition, the result of 193 nm photolysis (difference spectrum with the background after deposition), and the result of annealing at 50 K (difference spectrum with the background after photolysis). The band of CN is marked with a dot. The spectra were measured at 9 K. BrCN, BrNC, and BrXeCN are marked with V, VI, and VII, respectively.

species in argon and krypton matrixes.²⁷ Upon photolysis, the BrCN bands decrease in intensity, whereas two absorption bands appear in the mid-infrared region at 2061 cm^{-1} (absorber VI) and 2139 cm^{-1} (absorber VII) (Figure 2). The CN band at 2040 cm^{-1} also appears after photolysis. The 2061 cm^{-1} band (absorber VI) originates from BrNC as it is close to the band reported for this species in an argon matrix (2067 cm^{-1}).²⁹ The BrNC band in the far-infrared region is not detected, which is consistent with the very small theoretical intensity (B3LYP: 0.3 km mol^{-1}).

The 2139 cm^{-1} band (absorber VII) substantially increases upon annealing at 40–50 K (Figure 3), and it presumably originates from a Xe-containing molecule. We assign this band to BrXeCN. Indeed, it appears between the bands of BrCN and BrNC, similar to the previous case when the ClXeCN band is located between the ClCN and ClNC bands. The BrXeCN band (2139 cm^{-1}) is close to the ClXeCN band (2145 cm^{-1}), whereas the hypothetical band of BrXeNC should be considerably lower in frequency. In the far-infrared region, the corresponding band is observed at 297 cm^{-1} and its position agrees with the calculations for BrXeCN (B3LYP: 297 cm^{-1}). The formation of BrXeCN is reasonable based on the calculated energies (B3LYP: 1.2 eV lower than the 3B asymptote), whereas BrXeNC is substantially higher in energy (Table 2). Because of probable computational errors, the energy of BrXeNC may in reality be higher than the 3B energy asymptote even though it is theoretically 0.64 eV lower (B3LYP). It is also notable that BrXeNC is not found after photolysis even though the light-induced formation should be less sensitive to the energy of the molecule with respect to the 3B asymptote. This suggests that the energy barrier, which protects BrXeNC from decomposition, is probably quite low.

In this series of experiments, we tried to prepare similar molecules with krypton; however, no positive results were obtained. The lack of the formation of the krypton-containing molecules upon annealing of the photolyzed matrix is, in general, consistent with their relatively low stability with respect to the 3B asymptote predicted by the calculations (Table 2), although the formation of ClKrCN could be possible.

CONCLUSIONS

In the present work, we have identified three new noble-gas molecules ClXeCN, ClXeNC, and BrXeCN prepared in a xenon matrix. The experimental spectra agree well with the quantum chemical calculations for these species. The use of Br instead of Cl decreases the stability of these species because

only one isomer BrXeCN is found, whereas both ClXeCN and ClXeNC are identified. Similar molecules with krypton are not observed. The potential use of fluorine is promising for preparation of the corresponding krypton-containing molecule FKrCN. It would be interesting to test the formation of FXeCN isomers with respect to the puzzling failure to observe FXeH and FXeCCH. A promising direction for future work is to investigate molecules of the type YNgY' , where Y and Y' are arbitrary electronegative fragments. We believe that many other noble-gas molecules can be prepared in this way, possibly even with light noble gases.

ASSOCIATED CONTENT

Supporting Information

Calculated bond lengths of HalCN and HalNgCN isomers and full vibrational spectra of HalXeCN isomers (Hal = Cl and Br; Ng = Kr and Xe). This material is available free of charge via the Internet at <http://pubs.acs.org>.

AUTHOR INFORMATION

Corresponding Author

*E-mail: leonid.khriachtchev@helsinki.fi

Present Addresses

†Arthur Amos Noyes Laboratory of Chemical Physics, California Institute of Technology, 1200 East California Boulevard, Pasadena, California 91125, United States.

‡Georg-August-Universität, Institut für Physikalische Chemie, D-37077 Göttingen, Germany.

Notes

The authors declare no competing financial interest.

ACKNOWLEDGMENTS

This work was supported by the Finnish Centre of Excellence in Computational Molecular Science. A.V.D. acknowledges a postdoctoral grant from the Faculty of Science of the University of Helsinki (project No. 7500101). T.A. was a member of the graduate school LasKeMo. We thank the CSC – IT Center for Science Ltd. for computational resources and Harri Kiljunen for discussions on the synthesis of ClCN.

REFERENCES

- (1) Bartlett, N. *Proc. Chem. Soc., London* **1962**, 218.
- (2) Brel, V. K.; Pirgulyev, N. S.; Zefirov, N. S. *Usp. Khim.* **2001**, *70*, 262–298.
- (3) Lehmann, J. F.; Mercier, H. P. A.; Schrobilgen, G. J. *Coord. Chem. Rev.* **2002**, *233–234*, 1–39.
- (4) Grochala, W. *Chem. Soc. Rev.* **2007**, *36*, 1632–1655.
- (5) Turner, J. J.; Pimentel, G. C. *Science* **1963**, *140*, 974–975.
- (6) Howard, W. F.; Andrews, L. *J. Am. Chem. Soc.* **1974**, *96*, 7864–7868.
- (7) Khriachtchev, L.; Räsänen, M.; Gerber, R. B. *Acc. Chem. Res.* **2009**, *42*, 183–191.
- (8) McDowell, S. A. C. *Curr. Org. Chem.* **2006**, *10*, 791–803.
- (9) Lignell, A.; Khriachtchev, L. *J. Mol. Struct.* **2008**, *889*, 1–11.
- (10) Khriachtchev, L.; Tapio, S.; Domanskaya, A.; Räsänen, M.; Lundell, J. J. *Chem. Phys.* **2011**, *134*, 124307.
- (11) Khriachtchev, L.; Pettersson, M.; Runeberg, N.; Lundell, J.; Räsänen, M. *Nature (London)* **2000**, *406*, 874–876.
- (12) Khriachtchev, L.; Pettersson, M.; Lignell, A.; Räsänen, M. *J. Am. Chem. Soc.* **2001**, *123*, 8610–8611.
- (13) Pettersson, M.; Lundell, J.; Khriachtchev, L.; Räsänen, M. *J. Chem. Phys.* **1998**, *109*, 618–625.

- (14) Khriachtchev, L.; Tanskanen, H.; Cohen, A.; Gerber, R. B.; Lundell, J.; Pettersson, M.; Kiljunen, H.; Räsänen, M. *J. Am. Chem. Soc.* **2003**, *125*, 6876–6877.
- (15) Khriachtchev, L.; Tanskanen, H.; Lundell, J.; Pettersson, M.; Kiljunen, H.; Räsänen, M. *J. Am. Chem. Soc.* **2003**, *125*, 4696–4697.
- (16) Feldman, V. I.; Sukhov, F. F.; Orlov, A. Y.; Tyulpina, I. V. *J. Am. Chem. Soc.* **2003**, *125*, 4698–4699.
- (17) Tanskanen, H.; Khriachtchev, L.; Lundell, J.; Kiljunen, H.; Räsänen, M. *J. Am. Chem. Soc.* **2003**, *125*, 16361–16366.
- (18) Pettersson, M.; Khriachtchev, L.; Lundell, J.; Jolkkonen, S.; Räsänen, M. *J. Phys. Chem. A* **2000**, *104*, 3579–3583.
- (19) Khriachtchev, L.; Lignell, A.; Tanskanen, H.; Lundell, J.; Kiljunen, H.; Räsänen, M. *J. Phys. Chem. A* **2006**, *110*, 11876–11885.
- (20) Khriachtchev, L.; Domanskaya, A.; Lundell, J.; Akimov, A.; Räsänen, M.; Misochko, E. *J. Phys. Chem. A* **2010**, *114*, 4181–4187.
- (21) Frisch, M. J.; Trucks, G. W.; Schlegel, H. B.; Scuseria, G. E.; Robb, M. A.; Cheeseman, J. R.; Scalmani, G.; Barone, V.; Mennucci, B.; Petersson, G. A. et al. *Gaussian 09*, revision B.01; Gaussian, Inc.: Wallingford, CT, 2010.
- (22) Peterson, K. A.; Figgen, D.; Goll, E.; Stoll, H.; Dolg, M. *J. Chem. Phys.* **2003**, *119*, 11113–11123.
- (23) Glendenning, E. D.; Reed, A. E.; Carpenter, J. E.; Weinhold, F. *NBO*, Version 3.1.
- (24) Lignell, A.; Khriachtchev, L.; Lundell, J.; Tanskanen, H.; Räsänen, M. *J. Chem. Phys.* **2006**, *125*, 184514.
- (25) Bhattacharyya, I.; Bera, N. C.; Das, A. K. *Eur. Phys. J. D* **2007**, *42*, 221–226.
- (26) Coleman, G. H.; Leeper, R. W.; Schulze, C. C. *Inorg. Synth.* **1946**, *2*, 90–94.
- (27) Freedman, T. B.; Nixon, E. R. *J. Chem. Phys.* **1972**, *56*, 698–707.
- (28) Khriachtchev, L.; Pettersson, M.; Räsänen, M. *Chem. Phys. Lett.* **1998**, *288*, 727–733.
- (29) Milligan, D. E.; Jacox, M. E. *J. Chem. Phys.* **1967**, *47*, 278–285.
- (30) Khriachtchev, L.; Pettersson, M.; Lundell, J.; Räsänen, M. *J. Chem. Phys.* **2001**, *114*, 7727–7730.
- (31) Khriachtchev, L.; Tapio, S.; Räsänen, M.; Domanskaya, A.; Lignell, A. *J. Chem. Phys.* **2010**, *133*, 084309.
- (32) Pettersson, M.; Khriachtchev, L.; Lignell, A.; Räsänen, M.; Bihary, Z.; Gerber, R. B. *J. Chem. Phys.* **2002**, *116*, 2508–2515.